Fast microfluidic temperature control for high resolution live cell imaging†

Guilhem Velve Casquillas,[abd] Chuanhai Fu,[b] Mael Le Berre,[a] Jeremy Cramer,[a] Sebastien Meance,[d] Adrien Plecis,[d] Damien Baigl,[c] Jean-Jacques Greffet,[e] Yong Chen,[c] Matthieu Piel[a] and Phong T. Tran*[ab]

Received 21st July 2010, Accepted 3rd November 2010
DOI: 10.1039/c0lc00222d

One major advantage of using genetically tractable model organisms such as the fission yeast *Schizosaccharomyces pombe* is the ability to construct temperature-sensitive mutations in a gene. The resulting gene product or protein behaves as wildtype at permissive temperatures. At non-permissive or restrictive temperatures the protein becomes unstable and some or all of its functions are abrogated. The protein regains its function when returning to a permissive temperature. In principle, temperature-sensitive mutation enables precise temporal control of protein activity when coupled to a fast temperature controller. Current commercial temperature control devices do not have fast switching capability over a wide range of temperatures, making repeated temperature changes impossible or impractical at the cellular timescale of seconds or minutes. Microfabrication using soft-lithography is emerging as a powerful tool for cell biological research. We present here a simple disposable polydimethylsiloxane (PDMS) based microfluidic device capable of reversibly switching between 5 °C and 45 °C in less than 10 s. This device allows high-resolution live cell imaging with an oil immersion objective lens. We demonstrate the utility of this device for studying microtubule dynamics throughout the cell cycle.

Introduction

Live cell imaging using green fluorescent protein (GFP) or other genetically-encoded variants has served as a powerful tool for biologists to monitor protein dynamics in studying protein functions.[1–3] In addition, genetic model organisms have enabled the creation of temperature-sensitive mutations in genes which allow partial or complete inactivation of the function of those gene products at non-permissive temperatures, leading to new discoveries of gene functions.[4,5] Temperature sensitivity is based on the reversible temperature-dependent conformational instability of a protein of interest.[6] Temperature-sensitive mutants can be a powerful tool for precise temporal control of protein activity when coupled to live cell imaging, provided that there is a temperature control device capable of fast switching on the cellular timescales of seconds or minutes.

The most common method to perform temperature-controlled biological experiments on the microscope is to use an incubation box (*e.g.* glove box), which encase the whole microscope inside a temperature-controlled box. The box provides a uniform temperature field, but requires tens of minutes to stabilize its temperature. For faster temperature control one can also use a temperature-controlled microscope stage coupled with an objective lens heater/cooler which enables temperature changes on the timescale of minutes (*e.g.*, Bioptechs Objective Heater System), but which generates a strong thermal gradient across the cell sample (>3 °C). These types of devices cannot deliver temperatures below ambient. For temperature changes on the timescale of seconds, the most common solution involves a micro-perfusion system, but this method generates shear flow on the cell, and therefore is not adaptable to non-adherent cells, like yeast. Another solution, based on funneling large-scale liquid flow from a water bath to the objective lens and microscope stage, can reach temperatures below ambient.[7] However, this relatively large device can be cumbersome and difficult to implement and requires structural modifications to the objective lens and the microscope stage. It also takes on the timescale of minutes to shift the temperature.

The use of micro-technology offers a faster alternative to controlling temperature during biological experiments. Microfabrication using soft-lithography and molding of the elastomer polydimethylsiloxane (PDMS) is providing powerful tools for biologists to precisely control the cellular microenvironment, such as cell geometry, chemical gradient and temperature.[8–10] To date, there exist many microfabricated devices capable of rapidly changing from ambient temperature (~25 °C) to much higher and non-physiological temperatures (>100 °C).[11–18] The most common approaches involve the integration of metallic or ITO thin films.[19,20] These technologies use the Joule effect produced by the passage of an electric current through a resistive thin film. However, these devices can not shift to temperatures lower than ambient and involve costly technology, prohibitive for daily biological experimentation. Finally, a cell chemostat made of bilayer PDMS has been introduced for cell culturing and imaging.[21] This microfluidic device was designed to maintain cells at the desired temperature, but it was not optimized to perform fast temperature shifts. To date, no microfabricated devices have been reported to operate in the range of useful

[a]*Institut Curie, UMR 144 CNRS, Paris, 75005, France. E-mail: phong.tran@curie.fr*
[b]*University of Pennsylvania, Cell & Developmental Biology, Philadelphia, PA, 19104, USA*
[c]*Ecole Normale Supérieure, UMR 8640, 75231 Paris, France*
[d]*Laboratoire de Photonique et de Nanostructures, CNRS, 91460 Marcoussis, France*
[e]*Laboratoire Charles Fabry, Institut d'Optique, Universite Paris Sud, CNRS, 91127 Palaiseau Cedex, France*
† Electronic supplementary information (ESI) available: Fig. S1–S3. See DOI: 10.1039/c0lc00222d

biological temperatures, at cellular timescales, while simultaneously allowing high-resolution imaging of cells.

We propose here a method which takes advantage of fast temperature changes inherent on the small characteristic length of microfluidic devices and the transparency and ease of microfabrication offered by soft-lithography of PDMS. We present a simple disposable PDMS-based microfluidic device which can be used to confine cells for high resolution imaging under oil immersion objective lenses, while simultaneously enabling temperature switching between 5 °C and 45 °C within 10 s. We demonstrate the utility of the device at the two extremities of the biological temperature spectrum: by reversibly depolymerizing and repolymerizing fission yeast *Schizosaccharomyces pombe* microtubules during interphase by cooling, and reversibly inactivating and reactivating the temperature-sensitive mutant Cut7-25^{ts} during mitosis by heating. This simple and easy to implement device is anticipated to aid the general cell biological community in studying temperature-sensitive mutations or cells at a wide range of temperatures and at high spatiotemporal resolution.

Results

Device design

The device is composed of two layers of microchannels (Fig. 1A and Fig. S1†). The bottom layer contains the yeast cells and the top layer allows circulation of temperature-controlled water, without direct contact between the yeast and the flowing cold/hot water. To control the temperature of the fluid injected into the top channel, we use two external Peltier devices set at two different temperatures and plugged into a syringe pump. By changing the flow direction, the device is filled with water coming from either the cold Peltier or the hot Peltier. This makes it possible to quickly change the temperature of the water flowing into the top temperature channels and therefore the temperature of the bottom yeast channels.

Thermal characterization

We first characterized the thermal response of the cell channels. Temperature changes were strongly dependent on the liquid flow rate. At flow rates between 20 μL s^{-1} to 50 μL s^{-1} we achieved a plateau of temperature stability, with standard deviations less than 0.3 °C (Fig. 1B and 1C). Since the presence of a plateau indicates the robustness of our device to fluid flow variations, in subsequent experiments we will operate only with a flow rate situated on this plateau (>20 μL s^{-1}).

For typical biological experiments, we often used temperature shifts that started at ambient (~25 °C) and went to either colder or warmer. Temperature shifting from ambient 25 °C to 5 °C (Fig. 1D) or 25 °C to 5 °C takes less than 10 s. Our Peltier devices have a practical temperature range between 1 °C to 50 °C. Therefore, we can reliably temperature shift the full dynamic range between 5 °C to 45 °C in less than 10 s (Fig. 1H).

When the temperature control chamber is coupled to an oil immersion objective lens for live cell imaging, the heavy metal casing of the lens acted as a heat sink to dissipate the temperature of the chamber. We measured a modest temperature lost of less than 3 °C when the chamber was in contact with the objective lens *via* immersion oil (Fig. 1E). The relatively small amount of heat lost due to the oil immersion objective lens suggests that temperature loss is easily compensated by extending the Peltier setting by a couple of degrees. We next correlated the Peltier temperature with the device temperature, using both dry and oil-immersion objective lenses. Our temperature device responded linearly with the Peltier settings (Fig. 1F).

Finally, we generated sinusoidal temperature shifts from 5 °C to 45 °C with a frequency of 1 shift/min, demonstrating the robustness of the device (Fig. 1G), and its ability to shift from 5 °C to 45 °C in less than 10 s (Fig. 1H). Thus this PDMS-based disposable microfluidic temperature-control device can give reliable and reproducible temperature shifts ranging from any temperature in the 5 °C to 45 °C range in less than 10 s. This device is anticipated to be useful for biological experiments requiring a high degree of spatiotemporal control of the cellular temperature.

Biological validation

We first tested the device by depolymerizing the fission yeast microtubule cytoskeleton. Microtubules are composed of αβ-tubulin heterodimers. The polymerization kinetics of tubulin respond to temperature.[22] Phase diagrams showed that microtubules depolymerize completely at 10 °C at any tubulin concentration *in vitro*.[22] It is generally known that cells incubated on ice for 30 min will also depolymerize their microtubules. To precisely quantify cold-induced microtubule behavior, we examined tubulin polymerization kinetics in living yeast cells expressing GFP-Atb2p (tubulin) (Fig. 2A). The microtubule cytoskeleton began to depolymerize at temperatures below 16 °C (Fig. 2B), and was completely depolymerized at 6 °C (Fig. 2B). Time to complete depolymerization was dependent on cell size (Fig. 2C), and was achieved between 3–6 min (Fig. 2A and 2C). This process was reversible and microtubule re-polymerization was observed by reversing the temperature from 6 °C back to the ambient 22 °C (Fig. 2A). The total cell fluorescence of GFP-Atb2p is contributed by free tubulin in the cytoplasm (60%) and tubulin in the microtubule polymer (40%). These fluorescence signals and ratios changed with the cooling temperature (Fig. 2D), but returned to their initial ambient levels after reheating. Our results on cold-dependent depolymerization of microtubules in living cells are consistent with previous *in vitro* studies using purified tubulin.[22]

A second test of the device was to examine the fission yeast temperature-sensitive mutant Cut7-25^{ts}. Cut7p is the essential fission yeast kinesin-5 motor involved in spindle formation during mitosis.[23,24] The Cut7-25^{ts} mutant, at the non-permissive or restrictive temperature of 35 °C, fails to make a bipolar spindle and the cell dies with a monopolar spindle phenotype.[23,24] While the Cut7-25^{ts} mutant is reversible, the timescale of protein inactivity and reversibility are not known. We used the microfluidic temperature control device to shift prophase mitotic Cut7-25^{ts} mutant cells expressing GFP-Atb2p (Fig. 3A). Within 2 min after shifting from the permissive 22 °C to the restrictive 35 °C, the prophase spindle exhibited a collapsed aster-like pattern of microtubules, consistent with a monopolar spindle phenotype (Fig. 3B). In contrast, wildtype cells did not exhibit prophase spindle collapse at the elevated temperature, but instead continued to elongate their spindles. Within 3 min after reversing

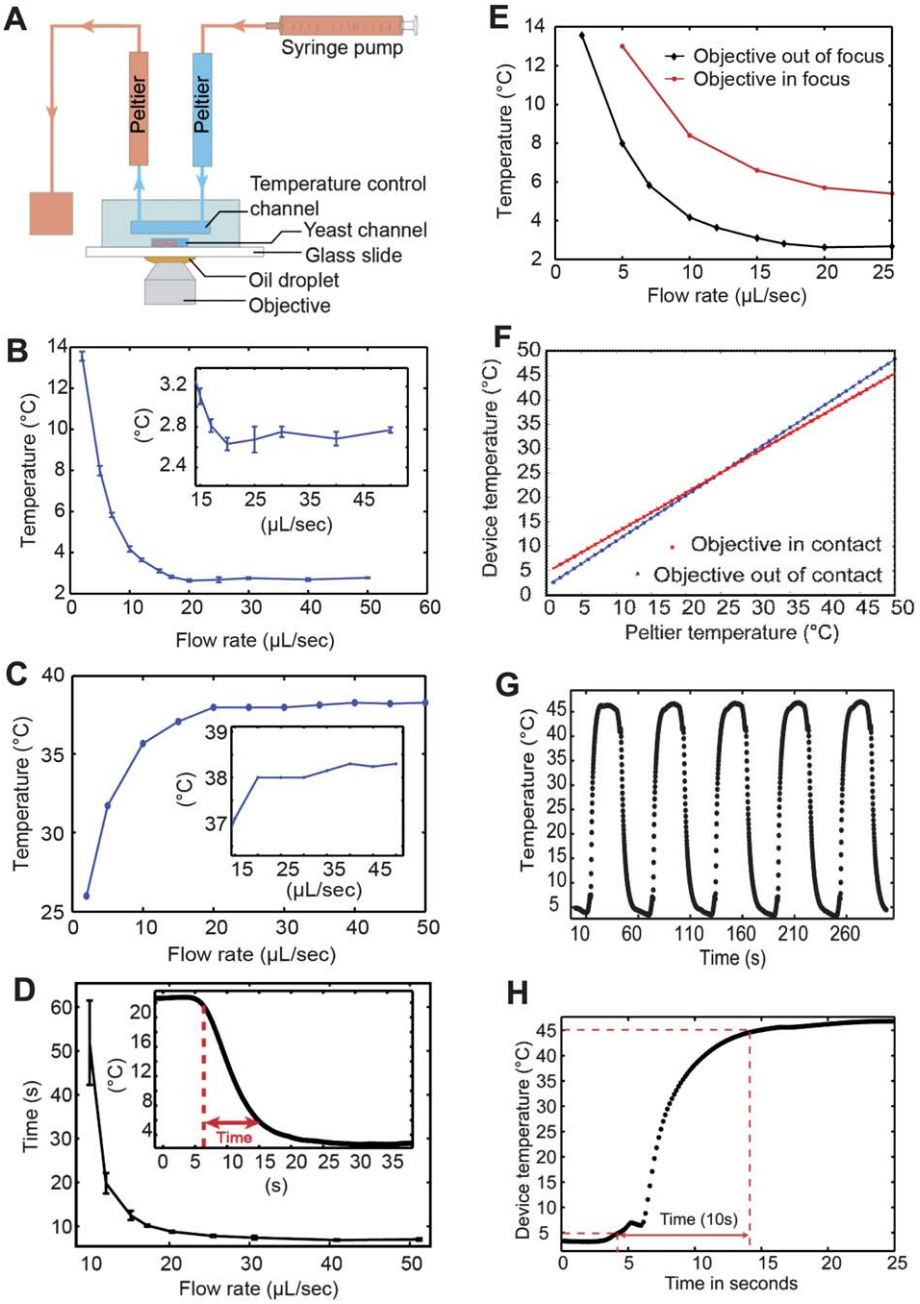

Fig. 1 Microfluidic temperature control device and its setup and validation. **A.** Schematic of the microfluidic temperature control device and setup. The Peltier controls the temperature of the liquid. The blue Peltier is set at the cold temperature and the red Peltier is set at the hot temperature. The cold–hot setting establishes the extremes or the temperature range. Changing the direction of the liquid flow through either cold or hot Peltier by the syringe pump changes the temperature experienced by the cells. **B**. Plot of cooling temperature *versus* flow rate. Peltier cold–hot setting was 1 °C and 26 °C. At a flow rate of 20 μL s^{-1} or higher, a temperature stability plateau is achieved at approximately 3 ± 0.3 °C ($N = 5$). **C**. Plot of heating temperature *versus* flow rate. Peltier cold and hot settings were 25 °C and 39 °C. At a flow rate of 20 μL s^{-1} or higher, a temperature stability is achieved at approximately 38 ± 0.3 °C ($N = 5$). **D**. Outside, plot of time *versus* flow rate to reach stable temperature. It takes less than 10 s at a flow rate of 20 μL s^{-1} or higher to shift to any desired temperature. Inside, plot of time *versus* temperature shifting at 20 μL s^{-1} flow rate and Peltier cold–hot setting was 1 °C and 23 °C. Shifting from 22 °C to 4 °C takes less than 10 s. **E**. Plot of temperature *versus* flow rate for oil immersion objective lens (red) and dry objective lens (blue). There is an approximate 3 °C loss due to oil immersion at all flow rates. **F**. Plot of correspondence temperature between Peltier and temperature device. Device temperature is given by the following equation: $T_{device} = T_{peltier} + A(T_{ambient} - T_{peltier})$; where $A = 0.071$ when the objective is in contact with the device cover slip; and $A = 0.187$ when objective is not in contact with the device cover slip. **G**. Plot of temperature *versus* time. Sinusoidal shifting between 5 °C and 45 °C is reversible and robust at 1 shift/min. **H**. Zoom-in of temperature *versus* time plot from Fig. 1G, showing the ability to shift from 5 °C to 45 °C in less than 10 s.

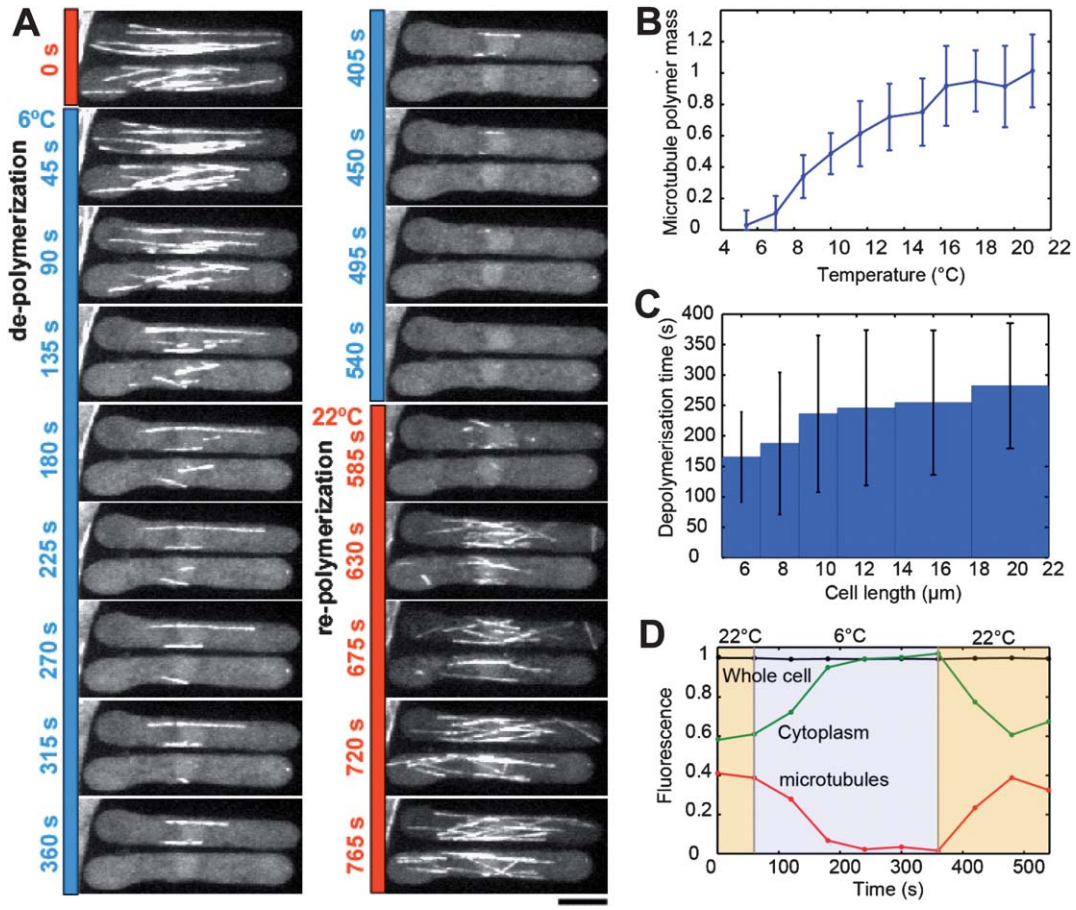

Fig. 2 Device validation by cooling cells. **A**. Interphase Cdc25-22 cells expressing GFP-Atb2p (tubulin). Cells were first imaged at ambient 22 °C, then shifted to 6 °C, then returned to 22 °C. Complete microtubule depolymerization occurs at 6 °C after several minutes, followed by microtubule repolymerization at 22 °C. Bar, 5 μm. **B**. Plot of normalized microtubule polymer mass *versus* temperature. Microtubule depolymerization starts at temperature below 16 °C. Complete microtubule depolymerization occurs at 6 °C ($N = 23$ cells). **C.** Plot of complete microtubule depolymerization time *versus* cell length. Longer cells have longer microtubules and take longer to depolymerize microtubules completely ($N = 117$ cells). **D**. Plot of normalized GFP-Atb2p (tubulin) fluorescence in microtubules (red), cytoplasm (green), and whole cell (black) during depolymerization and repolymerization temperature shifts ($N = 3$ cells). The ratio of tubulin in polymer form or cytoplasmic form changes with temperature.

back to the permissive ambient temperature, the Cut7-25^{ts} monopolar spindle reorganized into a proper bipolar spindle which continued to elongate through mitosis at the normal wildtype rate of 0.2 μm min^{-1} (Fig. 3B and 3C).[25] We conclude that the Cut7-25^{ts} mutant is a relatively fast-acting and reversible mutant, which can be precisely inactivated or reactivated within 2–3 min.

Discussion

We presented a simple, disposable, and fast PDMS-based microfluidic device capable of shifting cellular temperature in any range between 5 °C and 45 °C in less than 10 s. Due to the high precision and reproducibility of PDMS molding and spin coating technology it is not necessary to perform subsequent temperature characterization in replicate devices. For daily biological experimentation, our method enables the fabrication of a full glass/PDMS temperature control device without an integrated thin metallic film.

The temperature range of the device presented here (5–45 °C), which is suitable for many biological experiments, is mainly limited by the temperature range of the Peltier modules we used (0–50 °C). One can in principle use Peltier modules with higher temperature ranges, and replace water by the appropriate temperature conducting fluid, to reach temperatures below 0 °C or above 100 °C.

The current device can switch between two temperature points in less than 10 s. The main limitation for switching speed comes from the ability of the Peltier to maintain their internal temperature and from the fluid time constant of the system, *e.g.*, tubing length and insulation between the syringe pump and the Peltier module, and tubing length and insulation between the Peltier module and the microchannel. This limitation can be overcome with a more powerful Peltier and shorter tubing lengths.

The current device has temperature channels which are 100 μm thick and cell channels which are 5 μm thick. In practice, the system temperature calibration is applicable to all cell channel thicknesses when the thickness of the cell channel is small compared to the thickness of the temperature channel. For this

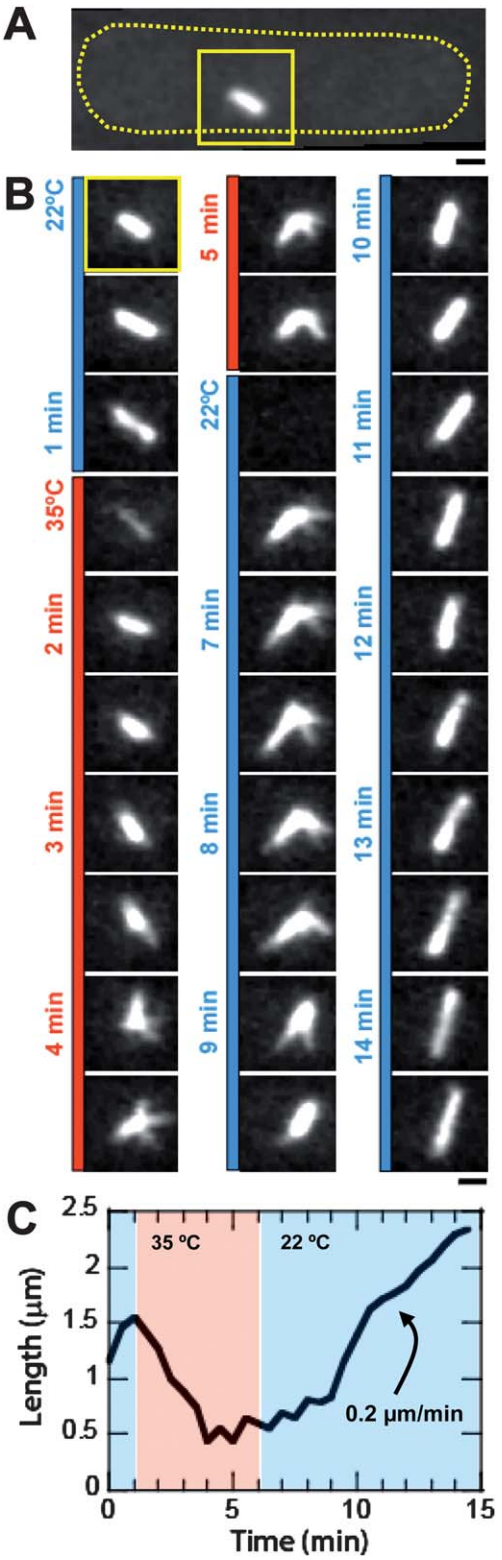

Fig. 3 Device validation by heating cells. **A**. Prophase mitotic Cut7-24^{ts} cell expressing GFP-Atb2p (tubulin). Yellow dotted line shows outline of a cell. A bipolar mitotic spindle at prophase is shown (inside yellow box). Bar, 1 μm. **B**. Time lapse images of the cell from A. The cell was first imaged at ambient 22 °C, where Cut7p is active. After shifting to the non-permissive temperature of 35 °C, the spindle quickly collapses into an aster pattern within 3 min, suggesting inactivation of Cut7p. Returning to 22 °C, the monopolar spindle aster quickly re-establishes bipolarity within 3 min and continues to elongate, suggesting Cut7p is active again. Bar, 1 μm. **C**. Plot of spindle length *versus* time during the temperature shift from the cell in B. The spindle elongation rate of 0.2 μm min^{-1} after reactivation of Cut7p is the same as wildtype,[25] suggesting full reactivation.

reason, our device and its temperature calibration would be relevant for cell channel thicknesses anywhere between 1 μm and 20 μm. Samples larger than 20 μm will require larger temperature channels and new calibration.

Conclusion

We anticipate that the ability to control the complete cellular microenvironment will be central to future cell biological studies. The emerging convergence of technologies from microfabrication, microscopy, and genetic model organisms has begun to revolutionize how cell biologists pose questions and has enabled cell biologists to be more quantitative in their analyses of biological processes.[26–28]

We presented here a disposable microfluidic device that enables fast temperature changes practical for biological experiments involving temperature-sensitive mutants and high spatiotemporal resolution imaging. The device is easy to fabricate and use in conventional cell biology laboratories and requires no modification to the current microscope setup. In addition, our device with two separate layers allows the cell layer to be adaptive, easily modifying cell shape or medium chemistry with new cell channel designs.[27] This device is anticipated to be of general utility to most cell biologists due to its ease of fabrication and use.

Methods

Device fabrication

The two layer chamber was fabricated using soft lithography and PDMS casting (Fig. S1†).[29–32] The master mold for the cell channels was created from a 5 μm thin SU8-2005 photoresist (www.microchem.com) patterned on a silicon wafer (www.silicon-wafers.com). The master mold for the temperature channels was created from a 100 μm thick SU8-2100 photoresist patterned on a silicon wafer. A mixture of 1 : 10 curing agent and PDMS was spin coated using the spin coater model CZ-650 (www.laurell.com) onto the cell mold at 6000 rpm to get a 10 μm thin PDMS replica. This step creates a 5–10 μm thin membrane on top of the cell channels. A mixture of 1 : 10 curing agent and PDMS was poured on the temperature mold, then released to get a 4 mm thick replica. Both temperature and cell PDMS replica were bonded together after 30 s plasma treatment using the Harrick Plasma Cleaner (www.harrickplasma.com). Inlets and outlets were drilled onto the PDMS block for fluidic connections. The block was finally bonded onto a glass cover slip after a 30 s plasma treatment.

Device setup

A computer controlled syringe pump model neMESYS (www.centoni.de), with a 30 mL plastic syringe was hooked in

series with inlet and outlet Peltier devices (Fig. 1A). The Peltier model was Warner SC-20 Peltier (www.warneronline.com), with controller model CL-100 (www.harvardapparatus.com). The connections between the Peltier and the PDMS chamber were done using 6 cm long Tygon tubing (ID, 0.51 mm). The 6 mm length tubing was calibrated for our specific setup. Longer tubing will require higher flow rate to compensate for the heat loss between Peltier and PDMS chamber.

Cells and microscopy

Two fission yeast strains were used for device validations: Cdc25-22/GFP-Atb2, and Cut7-24^{ts}/GFP-Atb2. Cell imaging was done as previously described.[33] Briefly, we used a Yokogawa CSU-10 spinning disc scan head coupled to a Nikon TE2000e inverted microscope (www.nikon.com). Cells were imaged in 3D with the 100×/1.45 NA objective lens and 488 nm laser illumination from a 25 mW Ag/Kr ion laser (www.mellesgriot.com). MetaMorph 7.5 (www.moleculardevices.com) controls the microscope and the Hamamatsu ORCA-AG CCD camera (www.hamamatsu.-com). All values are stated as mean ± standard deviation, with indicated N.

Thermal characterization

To characterize the temperature response of the chamber, we bonded the microchannel block to a "thermometer", which was made of 50 nm thin platinum resistance. This thermometer was made by photolithography and metal deposition directly onto the glass cover slip (Fig. S2†). The electrical resistance of platinum changes nearly linearly with temperature. We therefore measured the platinum electrical resistance to get the temperature of the platinum strip and thus deduce the temperature inside the cell channels.

The measurement was done using the 4-wires measurement method which enables the measurement of electrical resistance of a given portion of an electric resistor without the influence of the wire contact and the undesired area of the resistor[34] (Fig. S3A†). The shape of the platinum sensor was designed to measure the temperature only in the area containing the cell (Fig. S3B†). Three independents devices with embedded platinum resistance have been used for our characterization. All of them gave a similar result. All values are stated as mean ± standard deviation, with indicated $N = 10$ independent temperature switches.

Acknowledgements

We thank our respective lab members for helpful comments and suggestions. GVC, JC and FC performed experiments. GVC and PTT wrote the paper. All others contributed technological insights and equipment. GVC is supported by a traveling fellowship from JCS and a postdoctoral fellowship from ARC. This work is supported by grants from NIH, ACS, HFPS, FRM, ANR, MarieParis and LaLigue.

References

1 D. Muzzey and A. van Oudenaarden, *Annu. Rev. Cell Dev. Biol.*, 2009, **25**, 301–327.
2 K. I. Willig, R. R. Kellner, R. Medda, B. Hein, S. Jakobs and S. W. Hell, *Nat. Methods*, 2006, **3**, 721–723.
3 R. Yuste, *Nat. Methods*, 2005, **2**, 902–904.
4 G. Chakshusmathi, K. Mondal, G. S. Lakshmi, G. Singh, A. Roy, R. B. Ch, S. Madhusudhanan and R. Varadarajan, *Proc. Natl. Acad. Sci. U. S. A.*, 2004, **101**, 7925–7930.
5 G. Tan, M. Chen, C. Foote and C. Tan, *Genetics*, 2009, **183**, 13–22.
6 C. L. Gordon and J. King, *Genetics*, 1994, **136**, 427–438.
7 Y. Rabin and B. Podbilewicz, *J. Microsc.*, 2000, **199**, 214–223.
8 G. Velve-Casquillas, M. Le Berre, M. Piel and P. T. Tran, *Nano Today*, 2010, **5**, 28–47.
9 G. M. Whitesides, *Nature*, 2006, **442**, 368–373.
10 G. M. Whitesides, E. Ostuni, S. Takayama, X. Jiang and D. E. Ingber, *Annu. Rev. Biomed. Eng.*, 2001, **3**, 335–373.
11 H. F. Arata and H. Fujita, *Integr. Biol.*, 2009, **1**, 363–370.
12 H. Bridle, M. Millingen and A. Jesorka, *Lab Chip*, 2008, **8**, 480–483.
13 A. J. de Mello, M. Habgood, N. L. Lancaster, T. Welton and R. C. Wootton, *Lab Chip*, 2004, **4**, 417–419.
14 R. M. Guijt, A. Dodge, G. W. van Dedem, N. F. de Rooij and E. Verpoorte, *Lab Chip*, 2003, **3**, 1–4.
15 H. Kortmann, P. Chasanis, L. M. Blank, J. Franzke, E. Y. Kenig and A. Schmid, *Lab Chip*, 2009, **9**, 576–585.
16 T. Pennell, T. Suchyna, J. Wang, J. Heo, J. D. Felske, F. Sachs and S. Z. Hua, *Anal. Chem.*, 2008, **80**, 2447–2451.
17 D. Vigolo, R. Rusconi, R. Piazza and H. A. Stone, *Lab Chip*, 2010, **10**, 795–798.
18 T. Yamamoto, T. Fujii and T. Nojima, *Lab Chip*, 2002, **2**, 197–202.
19 M. Stangegaard, S. Petronis, A. M. Jorgensen, C. B. Christensen and M. Dufva, *Lab Chip*, 2006, **6**, 1045–1051.
20 C. Zhang, J. Xu, W. Ma and W. Zheng, *Biotechnol. Adv.*, 2006, **24**, 243–284.
21 A. Groisman, C. Lobo, H. Cho, J. K. Campbell, Y. S. Dufour, A. M. Stevens and A. Levchenko, *Nat. Methods*, 2005, **2**, 685–689.
22 D. K. Fygenson, E. Braun and A. Libchaber, *Phys. Rev. E: Stat. Phys., Plasmas, Fluids, Relat. Interdiscip. Top.*, 1994, **50**, 1579–1588.
23 I. Hagan and M. Yanagida, *Nature*, 1990, **347**, 563–566.
24 I. Hagan and M. Yanagida, *Nature*, 1992, **356**, 74–76.
25 I. Loiodice, J. Staub, T. G. Setty, N. P. Nguyen, A. Paoletti and P. T. Tran, *Mol. Biol. Cell*, 2005, **16**, 1756–1768.
26 S. Takeuchi, W. R. DiLuzio, D. B. Weibel and G. M. Whitesides, *Nano Lett.*, 2005, **5**, 1819–1823.
27 C. R. Terenna, T. Makushok, G. Velve-Casquillas, D. Baigl, Y. Chen, M. Bornens, A. Paoletti, M. Piel and P. T. Tran, *Curr. Biol.*, 2008, **18**, 1748–1753.
28 M. Thery, V. Racine, M. Piel, A. Pepin, A. Dimitrov, Y. Chen, J. B. Sibarita and M. Bornens, *Proc. Natl. Acad. Sci. U. S. A.*, 2006, **103**, 19771–19776.
29 J. C. McDonald, D. C. Duffy, J. R. Anderson, D. T. Chiu, H. Wu, O. J. Schueller and G. M. Whitesides, *Electrophoresis*, 2000, **21**, 27–40.
30 J. C. McDonald and G. M. Whitesides, *Acc. Chem. Res.*, 2002, **35**, 491–499.
31 S. R. Quake and A. Scherer, *Science*, 2000, **290**, 1536–1540.
32 S. K. Sia and G. M. Whitesides, *Electrophoresis*, 2003, **24**, 3563–3576.
33 P. T. Tran, A. Paoletti and F. Chang, *Methods*, 2004, **33**, 220–225.
34 P. R. N. Childs, J. R. Greenwood and C. A. Long, *Rev. Sci. Instrum.*, 2000, **71**, 2959–2978.